Mode-Resolved Phonon Transport in Twisted Graphene

Wenyang Ding(丁文扬)[1,2], Junichiro Shiomi[2*], and Bingyang Cao(曹炳阳)[1*]

[1]*Key Laboratory for Thermal Science and Power Engineering of Ministry of Education, Department of Engineering Mechanics, Tsinghua University, Beijing 100084, China*
[2]*Department of Mechanical Engineering, The University of Tokyo, Tokyo, Japan*

(Received 7 December 2025; accepted manuscript online 24 March 2026)

The influence of rotation angle on interlayer thermal transport in twisted graphene was investigated through mode-resolved atomistic Green's function. Thermal conductance exhibits a strong dependence on rotation angle, with the highest value at 0° and the lowest at 10°. Spectral transmission shows that twisted structures suppress high-frequency phonons (6–16 THz), while the untwisted case maintains higher transmission in the low-frequency range (0–6 THz). Mode-resolved results reveal that out-of-plane polarized phonons dominate interlayer heat conduction, whereas moiré-induced reconstruction hinders non-out-of-plane mode channels and enhances the relative contribution of out-of-plane phonon modes. Furthermore, incidence-angle-dependent transmission demonstrates that twisting particularly suppresses phonons with large incidence angles at high frequencies, and a distinct envelope pattern emerges at 30°. These findings highlight that twist angle effectively regulates phonon transmission pathways and interlayer thermal conductance, offering a practical approach for tuning heat transport in two-dimensional layered materials.

DOI: 10.1088/0256-307X/43/4/040801 CSTR: 32039.14.0256-307X.43.4.040801

The continuous downscaling of electronic devices has brought about severe local overheating, posing a fundamental limitation to both performance and reliability. Addressing this challenge requires the development of materials with intrinsically tunable thermal transport properties. Recently, two-dimensional (2D) materials have provided a versatile platform for property modulation, in which twisting between adjacent layers generates moiré patterns that profoundly reshape their electronic, optical, and thermal behaviors.[1–4] Among them, twisted bilayer graphene (TBG) has become a prototypical system; at the so-called magic angle (∼1.06°), flat electronic bands emerge,[5–8] giving rise to exotic correlated phenomena such as superconductivity,[9] the quantum anomalous Hall effect,[10] and orbital ferromagnetism.[11] Beyond the realm of quantum electronic phases, twist engineering has demonstrated remarkable capability in tuning band structures and enabling over 500% modulation of electronic conductivity.[9,12] While twist-angle-dependent electronic and optical properties have been extensively studied, their thermal transport counterparts remain far less understood, despite their crucial relevance to thermal management in 2D materials-based devices.[13,14]

Recent studies reveal that twisting can strongly alter phonon dispersion and phonon scattering, thereby modulating thermal conductivity of layered materials.[15–18] For instance, minimizing intrinsic helical twists in graphite yields a record through-plane conductivity of $13.4\,\mathrm{W{\cdot}m^{-1}{\cdot}K^{-1}}$.[19] In bilayer WS_2 and MoS_2, increasing twist angle suppresses thermal conductance due to modified interlayer interactions and reduced overlap of vibrational density of states.[20] Furthermore, both experimental and simulation studies of TBG reported a phonon polarizer effect, where thermal conductance can be modulated by as much as 631% with moiré angles due to strong tuning by the moiré pattern over the phonon transmission of high-frequency phonons.[21] These findings collectively establish twist engineering as a powerful route for controlling phonon transmission. However, the microscopic mode-resolved phonon transport analysis by twisting manipulation remains insufficiently elucidated, even though it is central to understanding and optimizing the twist-induced modulation of thermal conductivity.

The present work investigates mode-resolved phonon transmission in 2D materials using twisted graphene as a model system. Employing a mode-resolved atomistic Green's function (AGF) approach,[22–24] we calculate the out-of-plane thermal conductance of TBG at twist angles of 0°, 10°, 20°, and 30°. Our study constructs a coherent physical picture for twist-enabled phonon engineering and provides practical guidance for thermal management in 2D materials-based electronic, photonic, and thermoelectric devices.

A trilayer graphene structure was constructed, where a rotated graphene layer was sandwiched between two aligned graphene layers to generate different twist angles, as shown in Fig. 1. The rotation angles θ of 0°, 10°, 20°, and 30° are explored. The mode-resolved AGF has been performed for the computational analysis of phonon transport in twisted graphene systems. Due to the significant

*Corresponding authors. Email: shiomi@photon.t.u-tokyo.ac.jp; caoby@tsinghua.edu.cn

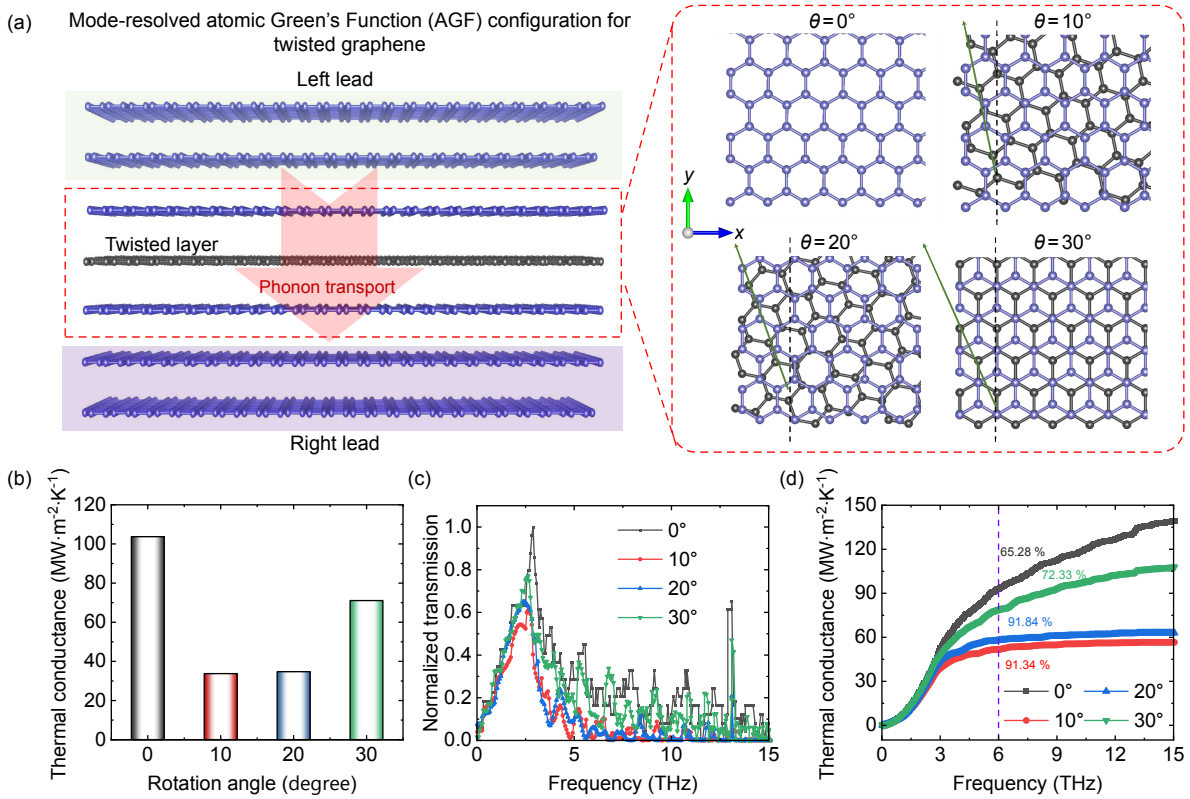

Fig. 1. (a) Mode-resolved atomistic Green's function configuration for twisted graphene and inset pictures are the atomic structures of twisted graphene with rotation angles of $\theta = 0°$, $\theta = 10°$, $\theta = 20°$, and $\theta = 30°$. (b) The calculated interfacial thermal conductance of twisted graphene at different rotation angles. (c) Spectral phonon transmission as a function of frequency for various rotation angles. (d) Cumulative thermal conductance versus frequency.

computational resources needed to compute the force-constant matrix, we opted to conduct mode-resolved AGF calculations on a smaller heterostructure with a reduced cross-sectional area. The unit cell parameters for twisted graphene systems are set to 4.310 Å × 2.491 Å. The configurations corresponding to these four angles result in unit cells of dimensions 12 × 18, 12 × 14, 16 × 8, and 12 × 18, respectively. The corresponding supercell areas are 51.76 Å × 44.82 Å, 51.99 Å × 34.71 Å, 68.95 Å × 19.90 Å, and 51.76 Å × 44.82 Å, respectively. The left and right leads consisted of an infinite array of double-layer graphene or graphite, whereas the center region consisted of trilayer twisted graphene. Then, the flux-normalized transmission matrix for phonon transmission from the left to the right lead can be calculated according to the mode-resolved AGF formalism in our previous work:[22–25]

$$\boldsymbol{t}_{\mathrm{RL}} = \frac{2\mathrm{i}\omega}{\sqrt{a_{\mathrm{L}}a_{\mathrm{R}}}} \boldsymbol{V}_{\mathrm{R}}^{1/2} [\boldsymbol{U}_{\mathrm{R}}^{\mathrm{ret}}]^{-1} \boldsymbol{G}^{\mathrm{ret}} [\boldsymbol{U}_{\mathrm{L}}^{\mathrm{adv}\dagger}]^{-1} \boldsymbol{V}_{\mathrm{L}}^{1/2}. \quad (1)$$

Here, $\boldsymbol{G}^{\mathrm{ret}} = g_{\mathrm{R}}^{00} \boldsymbol{H}^{\mathrm{RD}} \boldsymbol{G}_{\mathrm{D}}^{\mathrm{ret}} \boldsymbol{H}_{\mathrm{DL}} g_{\mathrm{L}}^{00}$, and $a_{\mathrm{L}}(a_{\mathrm{R}})$ is the length of the left (right) sublayer of lead. $\boldsymbol{V}_{\mathrm{L}}(\boldsymbol{V}_{\mathrm{R}})$ is the projection of the mode group velocity in the left (right) leads along the temperature gradient direction and are zero for evanescent phonons. $\boldsymbol{U}_{\mathrm{R}}^{\mathrm{ret}}(\boldsymbol{U}_{\mathrm{L}}^{\mathrm{adv}})$ is a matrix with its column vectors corresponding to the extended or decaying evanescent modes of right(left) lead. The modal transmission coefficient of the nth incoming phonon channel in the left lead is $\Xi_{\mathrm{L},n}(\omega) = [\bar{\boldsymbol{t}}_{\mathrm{RL}}^{\dagger} \bar{\boldsymbol{t}}_{\mathrm{RL}}]_{nn}$, and the spectral phonon transmission can be expressed as

$$\Xi(\omega) = \sum_{n=1}^{N_{\mathrm{L}}(+)} \Xi_{\mathrm{L},n}(\omega), \quad (2)$$

where $N_{\mathrm{L}}(+)$ represents the number of right-going phonon channels from the lead to the left side. The thermal conductance can be obtained through the Landauer formalism:[26,27]

$$\sigma(T) = \frac{1}{2\pi A} \int_0^{\omega_{\max}} \hbar\omega \frac{\partial n}{\partial T}(\omega, T)\, \Xi(\omega)\, \mathrm{d}\omega, \quad (3)$$

where A is the cross-sectional area, $n(\omega, T)$ is the Bose–Einstein distribution, and T is temperature.

The interfacial thermal conductance of twisted graphene with rotation angles of 0°, 10°, 20°, and 30° is shown in Fig. 1(b). The highest thermal conductance was observed at 0°, which decreased notably at 10°, slightly increased at 20°, and then increased again at 30°. The lowest interfacial thermal conductance is observed to be 56.65 MW·m^{-2}·K^{-1} at the rotation angle of 10°, resulting from the interplay between pronounced stress localization and enhanced interlayer coupling in enlarged AA regions governed by the increased moiré length,[16,17] as shown in Fig. S1 in Supplementary Materials. Moreover, the effects of temperature on the thermal conductance of twisted graphene with rotation angles of 0°, 10°, 20°, and 30° have been investigated; the thermal conductance of the four structures exhibits an upward trend. This behavior stems from the increased vibrational intensity of

atoms within the lattice as temperature rises; details can be found in Fig. S2. To further analyze phonon spectral information, we calculated the spectral phonon transmissions for twisted graphene with varied rotation angles in Fig. 1(c). It is evident that the spectral phonon transmission exhibits a strong dependence on rotation angle. The transmissions of all the twisted graphene systems show high peaks in the low-frequency range of 0–10 THz and fluctuate at frequencies above 10 THz. Notably, the transmission at the rotation angle of 0° (black squares) tends to be higher compared to the other angles, particularly in the 0–6 THz range. To quantitatively analyze the suppression of phonon transport under twisting, the cumulative thermal conductance is presented in Fig. 1(d). The contributions from phonons in the range of 0–6 THz account for only 65.28%, 91.34%, 91.84%, and 72.33% of the total thermal conductance at rotation angles of 0°, 10°, 20°, and 30°, respectively. In other words, compared with 0° and 30°, the transmissions at 10° and 20° are strongly suppressed in the high-frequency range (6–16 THz).

To further clarify the impact of rotation angle on mode-resolved phonon transmission, the modal contributions of graphene systems with $\theta = 0°$, 10°, 20°, and 30° are presented in Figs. 2(a)–2(d). In graphite, the interlayer interactions impose constraints that significantly stiffen the out-of-plane phonons, altering the dispersion relationship from quadratic (ZA in graphene) to linear (LA in graphite). The analysis reveals that the out-of-plane phonons of LA and LO dominate interlayer thermal transport across all twisted structures, while their contribution in the untwisted system ($\theta = 0°$) is relatively smaller, indicating that twisting alters the distribution of available transmission channels. Quantitatively, out-of-plane phonon modes account for about 99.7% of the spectral transmission in untwisted graphene, whereas their contributions are 100% at $\theta = 10°$, 20°, and 30°. These results are consistent with previous experimental and simulation studies,[21] where the dominance of out-of-plane modes is explained by their reduced scattering phase space, arising from the large energy gap between the out-of-plane LA and LO modes. In other words, the emergence of Moiré patterns in twisted graphene is found to significantly hinder the transport pathways of non-out-of-plane modes while preferentially allowing out-of-plane phonons to transmit heat, with the thermal transport efficiency strongly influenced by the degree of stacking commensurability.

To elucidate the effect of rotation angle on incidence-angle-dependent phonon transmission, the results for graphene systems with $\theta = 0°$, 10°, 20°, and 30° are shown in Fig. 3. The color gradient from brown to green reflects

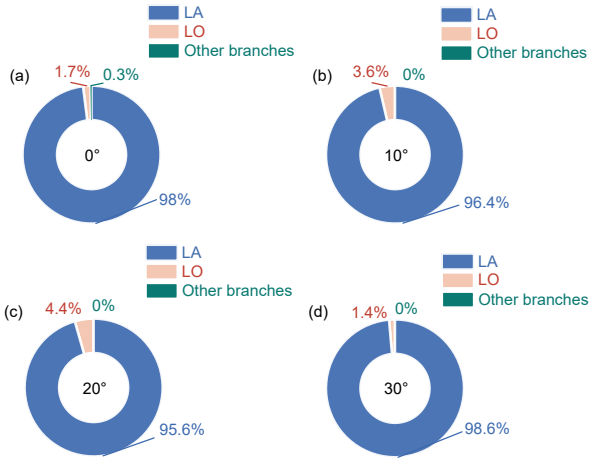

Fig. 2. The dependence of modal transmission contribution with four rotation angles: (a) $\theta = 0°$, (b) $\theta = 10°$, (c) $\theta = 20°$, (d) $\theta = 30°$.

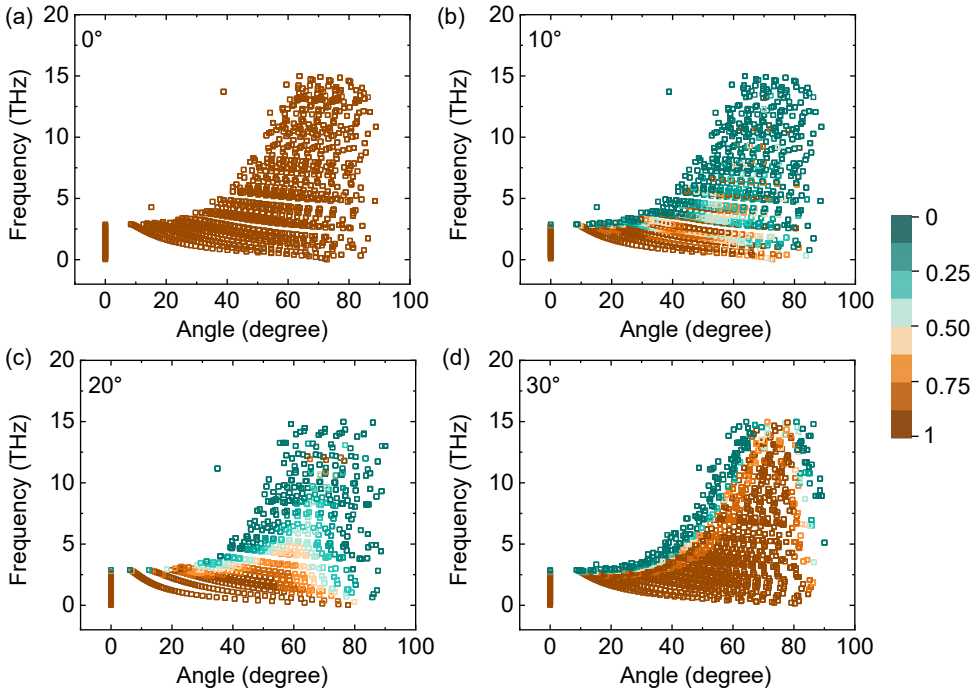

Fig. 3. The dependence of phonon modal transmission on angle of incidence and frequency with (a) $\theta = 0°$, (b) $\theta = 10°$, (c) $\theta = 20°$, and (d) $\theta = 30°$ rotation angles.

the transmission intensity, where brown indicates strong transmission and green denotes suppression of transmission. For the untwisted structure ($\theta = 0°$) in Fig. 3(a), all phonon modes exhibit full transmission, as evidenced by the uniform brown distribution. With increasing rotation angle to 10° and 20°, phonons at large incidence angles and high frequencies are markedly suppressed in Figs. 3(b) and 3(c), manifested as a progressive transition from brown to green in the transmission maps. At $\theta = 30°$, the distribution exhibits a distinctive feature in Fig. 3(d), where a green envelope surrounds a brown region, contrasting with the patterns at smaller twist angles. This behavior reveals that twisting significantly hinders high-frequency phonon transport at large incidence angles, while still allowing partial transmission channels to survive. Such modulation originates from the moiré-induced structural reconstruction, which strongly depends on the incidence angle and phonon frequency. Overall, these results highlight that twist angle provides an effective means to regulate incidence-angle-dependent phonon transmission, thereby tuning interlayer heat conduction in multilayer graphene.

In summary, the thermal conductance of twisted graphene exhibits a clear dependence on rotation angle, with the lowest value observed at 10°. Spectral transmission analysis demonstrates that twisting strongly suppresses high-frequency phonons, while mode-resolved results confirm the dominant role of out-of-plane modes in interlayer heat conduction. The emergence of moiré patterns further blocks non-out-of-plane phonon transmission channels and enhances the contribution of out-of-plane modes. Incidence-angle-dependent transmission reveals that twisting particularly hinders phonons with large incidence angles at high frequencies, and a unique envelope feature is observed at 30°. Overall, these findings reveal that twist angle effectively modulates phonon transmission pathways and out-of-plane thermal conductance, providing new perspectives for tailoring heat conduction in two-dimensional layered systems.

Acknowledgements. This research was funded by the National Natural Science Foundation of China (Grant Nos. 52506092, 52425601, and 52327809), the National Key Research and Development Program of China (Grant No. 2023YFB4404104), the Beijing Natural Science Foundation (Grant No. L233022), the China Postdoctoral Science Foundation (Grant No. 2025M770583), and the Shuimu Tsinghua Scholar Program of Tsinghua University.

References

[1] Geim A K and Grigorieva I V 2013 *Nature* **499** 419
[2] Manzeli S, Ovchinnikov D, Pasquier D, Yazyev O V, and Kis A 2017 *Nat. Rev. Mater.* **2** 17033
[3] Yang S, Zhang Y, Zhou C, and Yi H 2021 *Int. J. Therm. Sci.* **170** 107142
[4] Song J, Miao T, An M, and Chen D 2026 *Int. J. Heat Fluid Flow* **117** 110033
[5] Ahmed S, Alam S, and Jain A 2023 *Phys. Rev. B* **108** 235202
[6] Nimbalkar A and Kim H 2020 *Nano-Micro Lett.* **12** 126
[7] Yang F, Zhou W, Zhang Z, Huang X, Zhang J, Liang N, Yan W, Wang Y, Ding M, Guo Q, Han Y, Liu T H, Liu K, Zheng Q, and Song B 2025 *Phys. Rev. Lett.* **134** 146302
[8] Perebeinos V, Tersoff J, and Avouris P 2012 *Phys. Rev. Lett.* **109** 236604
[9] Cao Y, Fatemi V, Fang S, Watanabe K, Taniguchi T, Kaxiras E, and Jarillo-Herrero P 2018 *Nature* **556** 43
[10] Serlin M, Tschirhart C L, Polshyn H, Zhang Y, Zhu J, Watanabe K, Taniguchi T, Balents L, and Young A F 2020 *Science* **367** 900
[11] Sharpe A L, Fox E J, Barnard A W, Finney J, Watanabe K, Taniguchi T, Kastner M A, and Goldhaber-Gordon D 2019 *Science* **365** 605
[12] Ribeiro-Palau R, Zhang C, Watanabe K, Taniguchi T, Hone J, and Dean C R 2018 *Science* **361** 690
[13] Kim S E, Mujid F, Rai A, Eriksson F, Suh J, Poddar P, Ray A, Park C, Fransson E, Zhong Y, Muller D A, Erhart P, Cahill D G, and Park J 2021 *Nature* **597** 660
[14] Quan J, Linhart L, Lin M L, Lee D, Zhu J, Wang C Y, Hsu W T, Choi J, Embley J, Young C, Taniguchi T, Watanabe K, Shih C K, Lai K, MacDonald A H, Tan P H, Libisch F, and Li X 2021 *Nat. Mater.* **20** 1100
[15] Zhang L, Zhong Y, Li X, Park J H, Song Q, Li L, Guo L, Kong J, and Chen G 2023 *Nano Lett.* **23** 7790
[16] Ren W, Chen J, and Zhang G 2022 *Appl. Phys. Lett.* **121** 140501
[17] Ren W, Lu S, Yu C, He J, Zhang Z, Chen J, and Zhang G 2023 *Appl. Phys. Rev.* **10** 041404
[18] Ren W, Ouyang Y, Jiang P, Yu C, He J, and Chen J 2021 *Nano Lett.* **21** 2634
[19] Zhao L, Chen Z, Hu S, Zhi A, Wu J, Kang F, Tian X, Gu X, and Sun B 2026 *Matter* **9** 102382
[20] Xu B, An M, Masubuchi S, Li Y, Guo R, Machida T, and Shiomi J 2025 *Adv. Funct. Mater.* **35** 2422761
[21] Qin Z, Dai L, Li M, Li S, Wu H, White K E, Gani G, Weiss P S, and Hu Y 2024 *Adv. Mater.* **36** 2312176
[22] Ong Z Y 2018 *Phys. Rev. B* **98** 195301
[23] Ding W, Guo J, An M, Tsuda K, and Shiomi J 2025 *npj Comput. Mater.* **11** 158
[24] Ding W, Ong Z Y, An M, Davier B, Hu S, Ohnishi M, and Shiomi J 2024 *Nano Lett.* **24** 13754
[25] Yang H and Cao B 2023 *J. Appl. Phys.* **134** 155302
[26] Yang L, Latour B, and Minnich A J 2018 *Phys. Rev. B* **97** 205306
[27] Dhar A and Roy D 2006 *J. Stat. Phys.* **125** 801